Erosional scours around ancient submarine volcanoes and the onset of the Leeuwin Current, offshore Southern Australia

Christopher A-L. Jackson*

Esther R. Hunt-Stewart

Craig Magee

Basins Research Group (BRG), Department of Earth Science & Engineering, Imperial College, Prince Consort Road, LONDON, SW7 2BP, UK

**corresponding author email: c.jackson@imperial.ac.uk*

ABSTRACT

The Leeuwin Current is one of the most important ocean currents in the southern hemisphere; it samples the global thermohaline system via the Indonesian Gateway, and flows southwards from the north-western corner of Australia and thereafter eastwards into the Great Australian Bight. In the geological past, the current has contributed to climatic variations, vegetation patterns and the rate of chemical weathering in southern Australia, in addition to transporting low-latitude fauna to anomalously high latitudes. However, the timing of its initiation, especially along the southern margin of Australia, is poorly understood. In this study we use 2D seismic reflection data from offshore southern Australia to document a series of 10–90 m deep, up to 3 km wide erosional scours, and <50 m thick, sediment wave-like bodies that are developed throughout the middle Eocene-to-Recent, carbonate-dominated succession. We suggest that these features record the onset of bottom-current activity, which we speculate is related to the middle Eocene initiation of the Leeuwin Current. The scours are particularly well-developed at one specific stratigraphic level and define ‘moats’ that encircle the flanks of middle Eocene shield volcanoes. These moats are considered to document a pronounced period of current intensification or ‘waxing’ during the middle Miocene, which may have been associated with changes in ocean circulation patterns driven by the Miocene Global Optimum. The results of this seismic reflection-based study are consistent with results derived from other paleoceanographic proxies, thereby highlighting the key role that seismic reflection data have in understanding the occurrence, geographical distribution and significance of ancient ocean currents.

INTRODUCTION

Thermohaline circulation of the world’s oceans controls regional and global climate trends, and biodiversity in modern and ancient ocean environments (e.g., Wunsch, 2002; Rahmstorf, 2003). The modern Leeuwin Current is the longest and one of the most important ocean currents in the southern hemisphere, and it is unusual in that it flows southwards from the north-western corner of Australia and thereafter eastwards into the Great Australian Bight (GAB) (inset in Fig. 1A) (Cresswell and Golding, 1980). Warm, low-salinity waters derived from the South Equatorial Current, via the Indonesian Gateway, feed the Leeuwin Current and it is therefore connected to and samples the global thermohaline system (Feng et al., 2009). The Leeuwin Current contributes to climatic variations and vegetation patterns (e.g., Caputi, 2001; Feng et al., 2009), and continent-scale biodiversity patterns by transporting otherwise low-latitude fauna to anomalously high latitudes (e.g., Cann and Clarke, 1993; McGowran et al., 1997; Passlow et al., 1997).

The Quaternary development, extent and behaviour of the Leeuwin Current in the GAB is relatively well understood (Cresswell and Golding, 1980; Feng et al., 2009). In contrast, the initiation and the pre-Quaternary eastward 'reach' of the Leeuwin Current into the GAB is uncertain because, like many ancient ocean currents, it is traditionally studied by mapping sparse vertical and lateral variations in pelagic and neritic faunal assemblages (e.g., McGowran et al., 1997) or isotope analysis of calcareous foraminifera (e.g., von Blackenburg, 1999). Based on the analysis of temperature sensitive foraminifera, McGowran et al. (1997) suggested that the 'proto-Leeuwin Current' initiated in the GAB during the late middle Eocene in response to accelerated opening of the Southern Ocean. Furthermore, Feary and James (1995, 1998) used data from IODP Leg 182 to speculate that the encroachment of anomalously warm waters into the GAB during the middle Miocene was probably an early manifestation of the Leeuwin Current, perhaps related to the Miocene Climatic Optimum (e.g. Savin et al., 1975; Gourley and Gallagher, 2004). Based on data from IODP Leg 182, McGowran et al. (1997) speculated that the protrusion of the proto-Leeuwin Current along the southern Australia margin was responsible for the development of the 'Little Barrier Reef', a thick (350 m), laterally extensive (>475 km long), middle Miocene rimmed carbonate platform. Data from IODP Leg 182 thus suggests that the proto-Leeuwin also played a key role in the stratigraphic evolution of the GAB shelf margin during the Eocene-to-Recent. However, the stratigraphic expression of time-equivalent, basin-centre units, which should also record the initiation and influence of the Leeuwin Current, has yet to be documented.

Seismic reflection data, which image geological features associated with ocean current activity in the deep seas, provide an alternative but hitherto underutilised method for determining the presence and behaviour of ancient ocean currents at the basin-scale (e.g., Boldreel et al., 1998; Davies et al., 2001; Due et al., 2006; Hohbein et al., 2012). In this study we use 2D seismic reflection data to describe stratigraphic features in the Middle Eocene-to-Recent succession of the eastern GAB that may be related to and document Middle Eocene initiation of the proto-Leeuwin Current. Our data suggest that a major period of seabed incision occurred during the Miocene, potentially associated with a period of current 'waxing' in the Early Miocene. We suggest that seismic reflection data should be integrated with biostratigraphic and geochemical proxies to help provide an improved understanding of ancient ocean current circulation, and the potential impact this may have on past variations in climate and biodiversity.

GEOLOGICAL SETTING

The Ceduna Sub-basin formed in response to crustal extension and thermal subsidence during the Jurassic-to-Early Cretaceous and Early Cretaceous-to-Recent, respectively (Figs 1A and 1B). The uppermost part of the basin comprises a fully marine, early Middle Eocene-to-Recent, carbonate-dominated interval (Nullarbor Limestone; Fig. 1B) (Schofield & Totterdell, 2008). Scours, which are interpreted to have formed in response to erosion of the seabed by ocean currents, have previously been identified in the Nullarbor Limestone, although the age, origin and significance of the associated current has not been explored (Fig. 2) (Schofield & Totterdell, 2008; Jackson, 2012). Absolute water depths during the Middle Eocene-to-Recent have not been directly constrained within the study area, although Jackson (2012) speculated that a water depth of a few hundred metres was established during a major transgression in the latest Middle Eocene (see also McGowran, 1977; 1989; Shafik, 1983; 1990). This interpretation is consistent with water depth indicators provided by Eocene clinoforms developed along the northern basin margin during the Eocene (Feary and James, 1995, 1998; McGowran et al., 1997). The Ceduna Sub-basin lies outboard of the modern day shelf edge in water depths of 200–4000 m; the seabed in the study area is below the influence of the modern Leeuwin Current, which extends to depths of 300 m (Feng et al., 2009).

DATA AND METHODS

Our dataset consists of 109, time-migrated, zero-phased, 2D seismic reflection lines that have a cumulative line length of *c*. 13,000 km and cover an area of *c*. 44,000 km^2 in the Ceduna Sub-basin (Fig. 1A). The NW-trending lines are spaced 4–16 km and NE-trending lines are spaced 4–8 km (Fig. 2). The Gnarlyknots-1a borehole provides information on the age of four key seismic reflections (Horizons A–D; Figs 1B and 3). This borehole also contains wireline log, which indicates the Nullarbor Limestone has a p-wave velocity of 2100 m s^{-1}, thereby allowing the conversion of measurements in milliseconds two-way time (ms TWT) to metres (cf. Espurt et al., 2009). Extrusive igneous bodies were identified and mapped using the geometric and geophysical criteria outlined by Totterdell & Schofield (2008), Jackson (2012) and Magee et al., (2013). The scours are characterised by erosional surfaces that truncate and are onlapped by, underlying and overlying reflections respectively (Fig. 3). These surfaces are typically imaged on several seismic lines and, although the seismic data is only 2D, it is clear that they form ‘moats’ around the volcanic edifices (see below and Fig. 2).

SEISMIC-STRATIGRAPHIC FRAMEWORK AND SEISMIC FACIES

The base of Stratal Unit 1 (SU1) is defined by a high-amplitude, laterally-continuous, positive seismic reflection that defines the contact between the Pidinga Formation and the Nullarbor Limestone, or the contact between the Nullarbor Limestone and a series of shield volcanoes (Figs 1B and 3). SU1 comprises the lower part of the Nullarbor Limestone and is typically characterised by low-to-moderate amplitude, parallel-to-sub-parallel, very continuous reflections away from the volcanoes (Fig. 3). Within 2 km of the volcanoes, a series of gently-dipping (<4°) reflections are developed in SU1, and these locally display bilateral downlap onto the underlying reflections and thus define convex-up, 'mound-like' bodies (Figs 3A–B). These inclined reflections, which either dip either towards (Fig. 3A) or away (Figs 3C–D) from the volcanoes, typically overlie low-angle (<6°) erosional surfaces, which are up to 2 km wide and display up to 100 m of relief; these surfaces pass laterally into (seismically) conformable surfaces (Fig. 3).

The base of SU2 is locally defined by a major erosion surface (Horizon D; Figs 1–3). This surface defines a series of 'moats' adjacent (<3 km) to 15 of the 57 volcanoes in the Ceduna Sub-basin. The moats are only developed around volcanoes that have a summit height of >60 m and, more typically, >200 m. The moats have a relief of 10–90 m and their flanks dip from 0.1–6.1°. Some of the moats are asymmetric, consisting of a long, gently dipping outer margin inclined towards the volcanoes and a shorter, more steeply-dipping surface that dips away from the volcanoes (Figs 3B–D). Two types of seismic facies fill the moats: (i) high-amplitude, 'wavy' or 'hummocky' reflections, which have a relief of up to 50 m and a distance of 100–200 m between adjacent 'wave crests' (Fig. 3B); and (ii) low-to-high amplitude, gently-dipping (<2°), moderately discontinuous to laterally-continuous reflections (Fig. 3). The upper part of SU2 is dominated by low-to-high amplitude, flat-lying to gently-dipping (<2°), laterally-continuous reflections and packages of chaotic reflections, which are bound at their bases by erosional surfaces (Fig. 3).

INTERPRETATION

It is unlikely that intra-Nullarbor erosional features documented here formed in a subaerial environment based on the observation that they are developed in a fully marine succession, and that the water depth was at least several hundred metres during the middle Eocene (Jackson, 2012). Furthermore, deep-water gravity currents are unlikely to have formed the intra-Nullarbor Limestone erosion surfaces because: (i) the northern basin margin was carbonate-dominated and constructional at this time, and little bypass of sediment appears to have occurred (Feary and James, 1995, 1998); and (ii) deep-water gravity currents do not typically form circular, moat-like erosional structures.

Our preferred interpretation is that the erosion surfaces formed in response to ocean current-related incision of the seabed. The inclined and wavy reflections observed throughout the succession are interpreted as dip-oblique and dip-parallel sections, respectively, formed through sediment wave- or contourite-like deposits (cf. Rebesco and Stow, 2001; Stow et al., 2003; Hohbein et al., 2012). Based on the recovery of Eocene-age, warm-water microfauna from the Otway Basin, it is likely that warm waters related to a paleo-Leeuwin Current, rather than cold waters related to a paleo-Flinders Current (inset map in Fig. 1A), had the greatest influence in the GAB during the Eocene. We therefore speculate that the paleo-Leeuwin Current was likely responsible for the formation of the stratigraphic features developed in the Eocene-to-Recent succession of the Ceduna Sub-basin. The observation that relatively low-relief erosion surfaces are developed throughout the Nullarbor Limestone provides seismic-stratigraphic evidence for both late middle Eocene initiation of the proto-Leeuwin Current and, perhaps, episodic, eustatically driven fluctuations in the strength and thus erosion potential of the proto-Leeuwin Current (Feary and James, 1995). Our seismic-based observations thus support previous interpretations based solely on relatively sparse micropalaeontological evidence (Shafik, 1983; McGowran et al., 1997) or data from the basin margin (Feary and James, 1995).

Based on its apparent age and its association with anomalously large scours, we suggest that the major intra-Nullarbor Limestone erosion surface is the stratigraphic expression of a middle Miocene intensification or ‘waxing’ of the proto-Leeuwin Current. The restriction of these scours to the immediate flanks of and the lateral transition to correlative conformities with increasing distance from, the middle Eocene shield volcanoes, implies that these features formed syn-incision bathymetric highs that disturbed the velocity structure of the ocean currents. This resulted in an increase in current turbulence and seabed shear stresses, thereby enhancing the potential for localised erosion of the seabed (e.g., O'Reilly et al., 2003; MacLachlan et al., 2008; Callaway et al., 2009; Rollet et al., 2012). Enhanced incision during the Late Miocene may have occurred in response to a eustatic sea-level fall (Feary and James, 1995), which would potentially have resulted in lowering of the influence of the erosive ocean current.

IMPLICATIONS AND CONCLUSIONS

Paleooceanographic proxy data are: (i) expensive to collect and are typically only acquired on academic scientific cruises (e.g. IODP); (ii) areally limited and only collected from discrete stratigraphic intervals; and (iii) do not commonly provide a physical (i.e. stratigraphic) record of the initiation, extent and decay on oceanographic currents. Our study shows that seismic reflection data can image erosional and depositional features that provide a physical record and are related to the activity of ancient ocean currents. We demonstrate that, by placing these features into a broad chronostratigraphic framework, important insights into the onset of major ocean currents can be acquired. Importantly, our analysis suggests that the proto-Leeuwin Current initiated in the deep-water part of the GAB, offshore Southern Australia during the early Middle Eocene, and that a period of current 'waxing' occurred in the middle Miocene. These results indicate that seismic reflection data allow the investigation of basin-scale changes in circulation, complementing rather sparse micro-faunal evidence, and could thus be an essential part of the paleoceanographer's toolkit. For example, future work should focus on detailed mapping of seismic reflection datasets from, for example, the western Bight Basin and Otway Basin; this may reveal similar, age-equivalent current-formed stratigraphic features, thus raising the possibility that the proto-Leeuwin Current extended further eastwards and influenced faunal distribution and potentially climate over a wider area than is currently assumed. Seismic-based studies would thus complement the rather sparse micro-faunal evidence.

ACKNOWLEDGEMENTS

Geoscience Australia are thanked for providing seismic and borehole data.

REFERENCES

Boldreel, L.O.L., Andersen, M.S., and Kuijpers, A., 1998, Neogene seismic facies and deep-water gateways in the Faeroe Bank area, NE Atlantic: Marine Geology, v. 152, p. 129-140.

Callaway, A., Smyth, J., Brown, C.J., Quinn, R., Service, M., and Long, D., 2009, The impact of scour processes on a smothered reef system in the Irish Sea: Estuarine, Coastal and Shelf Science, v. 84, p. 409–418.

Caputi, N., Chubb, C.F., and Pearce, A., 2001, Environmental effects on recruitment of the western rock lobster, Panulirus Cygnus: Marine and Freshwater Research, v. 52, p. 1167-1175.

Cann, J.H., and Clarke, J.A.D., 1993, The significance of *Marginopora vertebralis* Foraminifera in surficial sediments at Esperance, Western Australia and in last interglacial sediments in northern Spencer Gulf: Marine Geology, v. 111, p. 171–187.

Cresswell, G., and Goldring, T., 1980, Observations of a south-flowing current in the southeastern Indian Ocean: Deep Sea Research Part 1: Oceanographic Research Papers, v. 27, p. 449-466.

Davies, R.J., Cartwright, J.A., Pike, J., and Line, C., 2001, Early Oligocene initiation of North Atlantic deep water formation: Nature, v. 410, p. 917-920.

Due, L., van Aken, H.M., Boldreel, L.O., and Kuijpers, A., 2006, Seismic and oceanographic evidence of present-day bottom-water dynamics in the Lousy Bank-Hatton Bank area, NE Atlantic. Deep Sea Research Part 1: Oceanographic Research Papers, v. 53, p. 1729-1741.

Espurt, N., Callot, J-P., Totterdell, J., Struckmeyer, H., and Vially, R., 2009, Interaction between continental breakup dynamics and large-scale delta system evolution: insights from the Cretaceous Ceduna delta system, Bight Basin, southern Australian margin: Tectonics, v. 28, TC6002.

Feary, D.A., and James, N.P., 1995, Cenozoic biogenic mounds and buried Miocene (?) barrier reef on a predominantly cool-water carbonate continental margin, Eucla Basin, western Great Australian Bight: Geology, v. 23, p. 427-430.

Feary, D.A., and James, N.P., 1998, Seismic Stratigraphy and Geological Evolution of the Cenozoic, Cool-Water Eucla Platform, Great Australian Bight: AAPG Bulletin, v. 82, p. 792-816.

Feng, M., Waite, A., and Thompson, P., 2009, Climate variability and ocean production in the Leeuwin Current system off the west coast of Western Australia: Journal of the Royal Society of Western Australia, v. 92, p. 67-81.

Gourley, T.L., and Gallagher, S.J, 2004, Foraminiferal biofacies of the Miocene warm to cool climatic transition in the Port Phillip Basin, southeastern Australia: Journal of Foraminiferal Research, v. 34, p. 294-307.

Hohbein, M., Sexton, P.F., and Cartwright, J.A., 2012, Onset of North Atlantic Deep Water production coincident with inception of the Cenozoic global cooling trend: Geology, v. 40, p. 255-258.

Jackson, C.A-L., 2012, Seismic reflection imaging and controls on the preservation of ancient sill-fed magmatic vents: Journal of the Geological Society, v. 169, p. 503-506.

MacLachlan, S.E., Elliott, G.M., and Parsons, L.M., 2008, Investigations of the bottom current sculpted margin of the Hatton Bank, NE Atlantic: Marine Geology, v. 253, p. 170-184.

Magee, C., Hunt-Stewart, E., and Jackson, C.A-L., 2013, Volcano growth mechanisms and the role of sub-volcanic intrusions: Insights from 2D seismic reflection data: Earth and Planetary Science Letters, 373, p. 41-53.

McGowran, B., Qianyu, L., Cann, J., Padley, D., McKirdy, D.M., and Shafik, S., 1997, Biogeographic impact of the Leeuwin Current in southern Australia since the late Middle Eocene: Palaeogeography, Palaeoclimatology, Palaeoecology, v. 136, p. 19-40.

O'Reilly, B., Readman, P.W., Shannon, P.M., and Jacob, A.W.B., 2003, A model for the development of a carbonate mound population in the Rockall Trough based on deep-towed sidescan sonar data: Marine Geology, v. 198, p. 55-66.

Rahmstorf, S., 2003, The current climate: Nature, v. 421, p. 699.

Rebesco, M., and Stow, D., 2001, Seismic expression of contourites and related deposits: a preface: Marine Geophysical Researches, v. 22, p. 303–308.

Rollet, N., McGiveron, S., Hashimoto, T., Hackney, R., Petkovic, P., Higgins, K., Grosjean, E., Logan, G.A., 2012, Seafloor features and fluid migration in the Capel and Faust basins, offshore eastern Australia: Marine and Petroleum Geology, v. 35, p. 269–291.

Savin, S.M., Douglas, R.G., and Stehli, F.G., 1975, Tertiary marine paleotemperatures: Geological Society of American Bulletin, v. 86, p. 1499–1510.

Schofield, A., and Totterdell, J., 2008, Distribution, timing and origin of magmatism in the Bight and Eucla basins: Australian Government Report, 2008/24.

Shafik, S., 1983, Calcareous nannofossil biostratigraphy: an assessment of foraminiferal and sedimentation events in the Eocene of the Otway Basin, southeastern Australia: Journal of Australian Geology and Geophysics, v. 8, p. 1-17.

Shafik, S., 1990, The Maastrichtian and early Tertiary record of the Great Australian Bight Basin and its onshore equivalents on the Australian southern margin: a nannofossil study: Bureau of Mineral Resources Journal of Australian Geology and Geophysics, v. 11, p. 473-497.

Stow, D.A.V., Faugères, J.C., Howe, J.A., Pudsey, C.J., and Viana, A.R., 2003, Bottom currents, contourites and deep-sea sediment drifts: Current state-of-the-art, in Stow, D.A.V., et al., eds., Deep-water contourite systems: Modern drifts and ancient series, seismic and sedimentary characteristics: The Geological Society of London Memoir, v. 22, p. 73–84.

von Blanckenburg, F., 1999, Palaeoceonography: tracing past ocean circulation?: Science, v. 286, p. 1862-1863.

Wunsch, C., 2002, What is the thermohaline circulation?: Nature, v. 298, p. 1179-1181.

FIGURE CAPTIONS

Fig 1. (A) Map illustrating the geographical setting of the study area. The area covered by 2D seismic reflection data is outlined by a solid black line. Inset shows the key modern oceanographic currents developed along the western and southern Australian margin. LC=Leeuwin Current; ACC=Antarctic Circumpolar Current; WAC=West Australia Current;

FC=Flinders Current. OB=Otway Basin. (B) Simplified stratigraphic column based on data from boreholes Gnarlyknots-1A and Potoroo-1. Key seismic horizons (A–D) and seismic units (SU1-2) are indicated. The stratigraphic occurrence of intrusion and extrusive components of the Bight Basin Igneous Complex (BBIC) are shown.

Fig. 2. Time-structure map of the Horizon D merged with a time-structure map of Horizon C; this illustrates the distribution of volcano summits (labelled 'v' and encircled by a solid white line) that rise above Horizon D, and intra-SU2 moats (labelled 'm'). sw=sediment wave crests. (A) and (B) are from the southern and northern parts of the study area respectively. See Figure 1A for location of map. Light grey lines indicate seismic reflection profiles.

Fig. 3. (A)–(D) Interpreted seismic profiles illustrating the geometry, scale and relationship between extrusive volcanic features of the Bight Basin Igneous Complexes and intra-Nullabor Limestone scours (moats) and bedforms. Locations of the seismic lines are shown in Figure 2. Uninterpreted versions of sections are available in DRI1.

Fig. 4. (A–C) Schematic diagrams illustrating the evolution of intra-Nullarbor Limestone scours in the Great Australia Bight. The vertical dashed line in the 'current strength' column indicates the threshold for sediment erosion/non-deposition; these conditions occur at the onset of T2.

Data Repository Item (DR1). Uninterpreted versions of the seismic profiles presented in Fig. 3.

Fig. 1

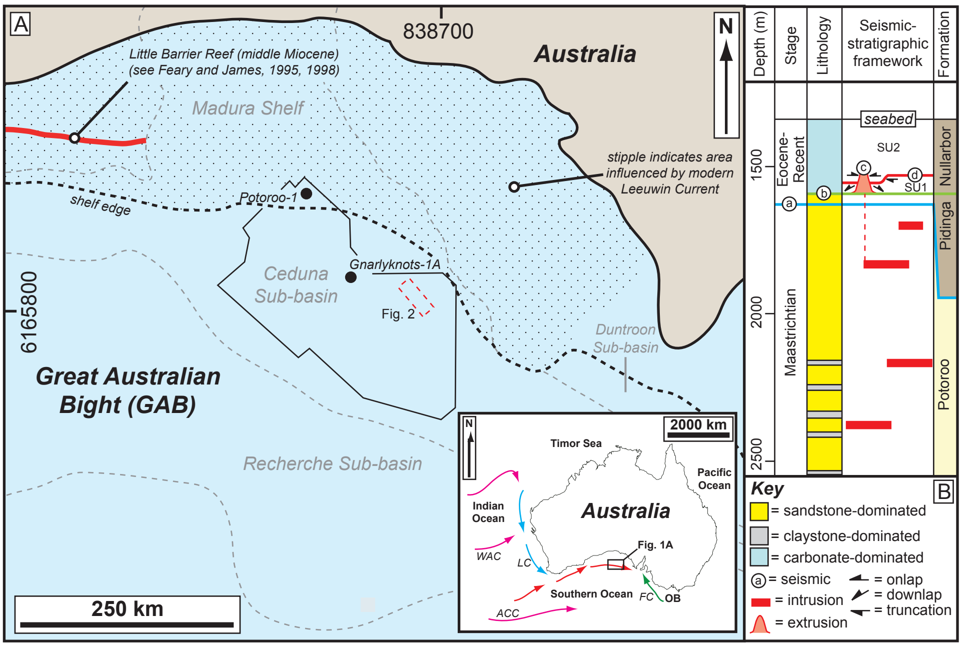
A
838700
Australia
N
Little Barrier Reef (middle Miocene)
(see Feary and James, 1995, 1998)
Madura Shelf
stipple indicates area influenced by modern Leeuwin Current
shelf edge
Potoroo-1
Gnarlyknots-1A
Ceduna Sub-basin
Fig. 2
Duntroon Sub-basin
6165800
Great Australian Bight (GAB)
Recherche Sub-basin
250 km
2000 km
Timor Sea
Pacific Ocean
Indian Ocean
Australia
WAC
LC
Fig. 1A
Southern Ocean
FC
OB
ACC
Depth (m)
Stage
Lithology
Seismic-stratigraphic framework
Formation
seabed
SU2
SU1
1500
2000
2500
Eocene-Recent
Maastrichtian
Nullarbor
Pidinga
Potoroo
Key
B
= sandstone-dominated
= claystone-dominated
= carbonate-dominated
= seismic
= intrusion
= extrusion
= onlap
= downlap
= truncation

Fig. 2

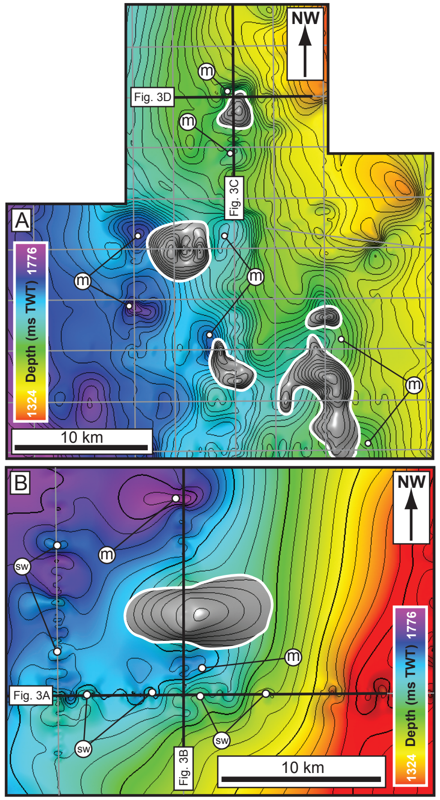

A
NW
Fig. 3D
Fig. 3C
m
Depth (ms TWT)
1324
1776
10 km
B
NW
sw
m
Fig. 3A
Fig. 3B
10 km

Fig. 3

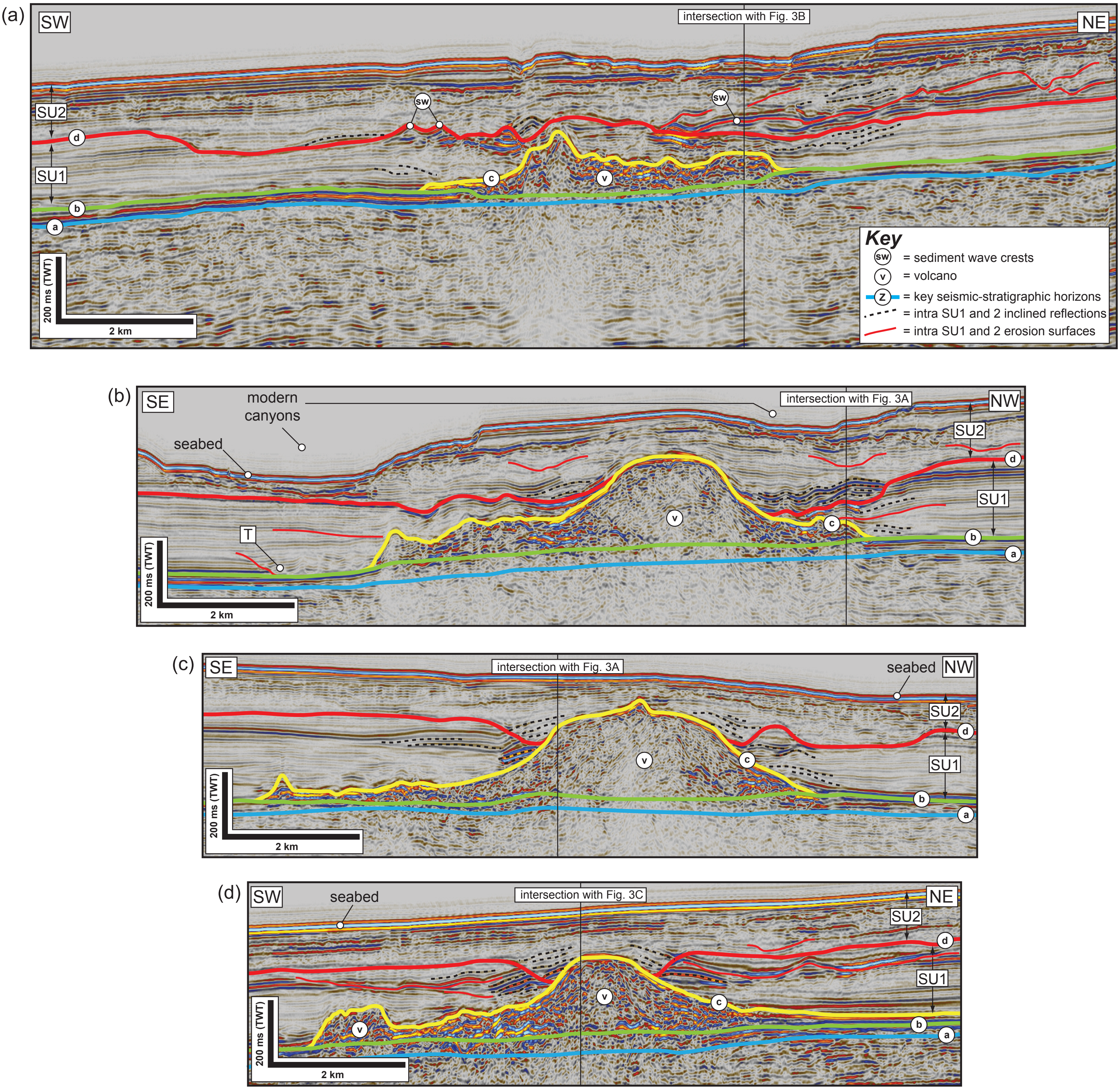
(a)
SW
NE
intersection with Fig. 3B
SU2
SU1
sw
d
c
v
b
a
200 ms (TWT)
2 km
Key
= sediment wave crests
= volcano
= key seismic-stratigraphic horizons
= intra SU1 and 2 inclined reflections
= intra SU1 and 2 erosion surfaces
(b)
SE
NW
modern canyons
seabed
intersection with Fig. 3A
T
(c)
SE
NW
intersection with Fig. 3A
seabed
(d)
SW
NE
seabed
intersection with Fig. 3C

Fig. 4

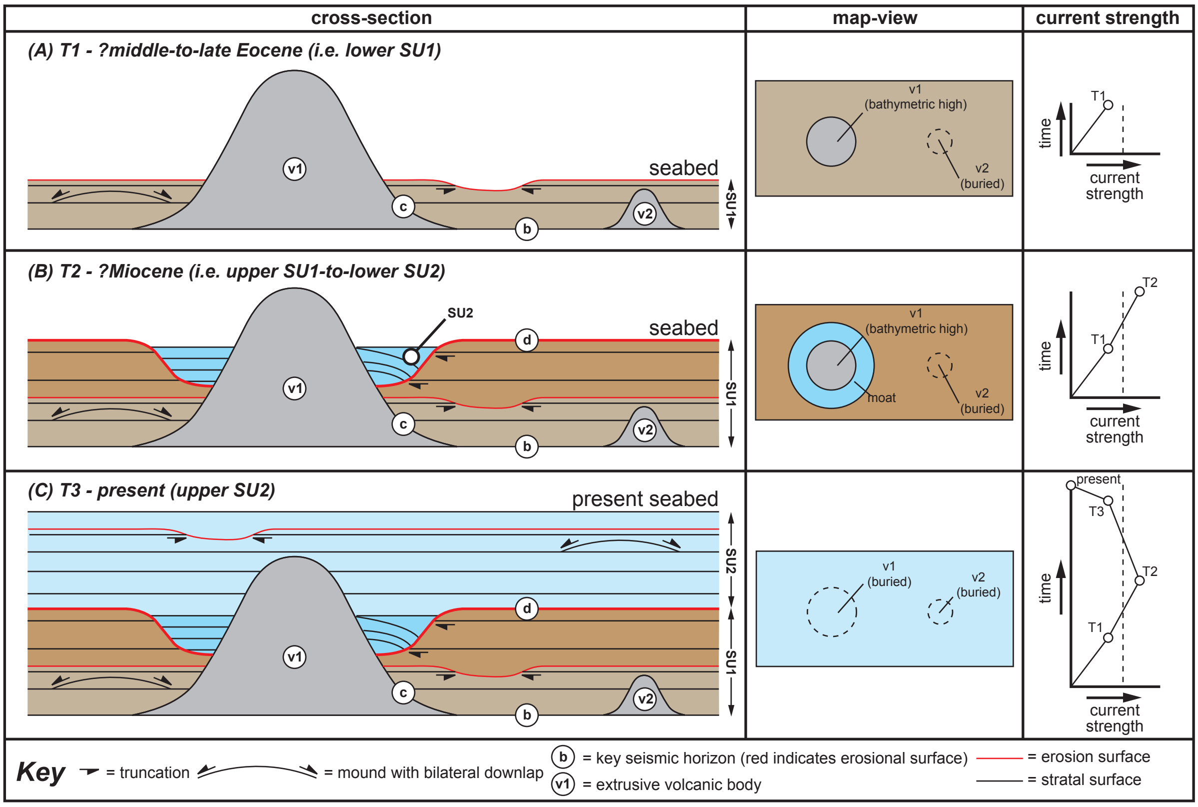

cross-section
map-view
current strength
(A) T1 - ?middle-to-late Eocene (i.e. lower SU1)
seabed
v1
c
b
v2
SU1
v1
(bathymetric high)
v2
(buried)
time
T1
current
strength
(B) T2 - ?Miocene (i.e. upper SU1-to-lower SU2)
SU2
seabed
d
v1
c
b
v2
SU1
moat
T2
(C) T3 - present (upper SU2)
present seabed
SU2
v1
(buried)
v2
(buried)
present
T3
Key
= truncation
= mound with bilateral downlap
b = key seismic horizon (red indicates erosional surface)
v1 = extrusive volcanic body
= erosion surface
= stratal surface